THE EFFECT OF FOULING ON HEAT TRANSFER, PRESSURE DROP AND THROUGHPUT IN REFINERY PREHEAT TRAINS: OPTIMISATION OF CLEANING SCHEDULES

E. M. Ishiyama, W. R. Paterson, D. I. Wilson

Department of Chemical Engineering, Pembroke Street, Cambridge CB2 3RA, UK E-mail: emi22@cam.ac.uk

ABSTRACT

Optimising cleaning schedules for refinery preheat trains requires a robust and reliable simulator, reliable fouling models and the ability to handle the thermal and hydraulic impacts of fouling. The interaction between thermal and hydraulic effects is explored using engineering analyses and fouling rate laws based on the 'threshold fouling' concept; the potential occurrence of a new phenomenon, 'thermo-hydraulic channeling' in parallel heat exchangers, is identified. The importance of the foulant thermal conductivity is highlighted. We also report the development of a highly flexible preheat train simulator constructed in MATLAB™/Excel™. It is able to accommodate variable throughput, control valve operation and different cost scenarios. The simulator is demonstrated on a network of 14 heat exchangers, where the importance of optimising the flow split between parallel streams is illustrated.

INTRODUCTION

Refineries employ series of heat exchangers in preheat trains (PHTs) to recover heat from the products of fractional distillation and thereby reduce the energy demand and the capital and operating costs. The effect of fouling on the performance of heat exchangers (HEs) in PHTs has been discussed at length previously (*e.g.* ESDU, 2000). Over the last decade the industry has moved from treating fouling as a chronic problem (to be lived with) to one which should be treated and, where possible, eliminated. The factors driving this change include the environmental impact of increased furnace firing to compensate for lost efficiency, the increase in crude price (and therefore the need to use less of each barrel to fuel its processing), the desire to maximize capacity utilization and the need to minimize refinery operating costs.

Fouling mitigation strategies include (i) adding antifoulant chemicals to the crude feed to eliminate or reduce the rate of fouling; (ii) modifying individual exchangers to render them more robust towards cleaning (including the use of extra area, flow inserts or replacement with fluidized bed designs); (iii) modifying the PHT network to optimize the temperature and flow conditions so as to reduce or minimize fouling at source; and (iv) periodic cleaning of fouled exchangers in order to maintain operability and meet targets. The development of quantitative models for fouling rates including temperature and flow effects, such as the 'threshold fouling' approach proposed by Ebert and Panchal (1997), has allowed workers to make considerable progress on hardware and operating options (ii)-(iv), as summarized by Wilson *et al*. (2005). Since the initial work by Smaïli and co-workers (*e.g*. Angadi *et al*., 1999), the PHT cleaning problem has attracted the attention of the numerical optimization community (Georgiadis *et al*., (2000); Lavaja, J.H. and Bagajewicz (2004/5); Sanaya and Niroomand, 2007) although their linear and non-linear programming (MILP, MINLP) techniques are not widely used at present. Even when plant data are used to give an estimate of local fouling rates, these numerical codes are criticized because the problems solved are idealized in critical respects. Another challenge is that the 'scheduling problem' has multiple solutions, with similar values of objective function, as shown in Figure 1. Smaïli *et al*. (2001) suggest that simpler optimization techniques such as the 'greedy algorithm', are adequate, particularly as they permit the use of simulations that encapsulate operating features that would cause stability problems in a 'total horizon' approach. Such operating features include varying throughput rates and splitter ratios (to minimize the impact of fouling, particularly when a unit is removed for cleaning).

Network simulation is essential for assessing any hardware modification to a PHT, as both the hydraulic and thermal performance of the system will be affected by changes in strategies (ii)-(iv). Yeap *et al*. (2005) have demonstrated that existing retrofitting techniques that use pinch technology typically rely on 'clean' performance estimates and ignore the dynamics resulting from fouling: they yield poorly performing networks. As a graphical technique to guide retrofit design, they developed the 'modified field plot', which encapsulates thermal and hydraulic aspects of fouling (Yeap *et al*., 2004). They demonstrated its application with case studies using relatively simple simulations. Variable throughput scenarios were not considered in detail. The current project builds on this prior work and considers the 'flow problem', wherein the mass flow rates in the network – which in the current operating climate of maximizing production is a key factor – are incorporated via hydraulic limitations and split fractions. A simulator has been constructed in MATLAB™/Excel™ for use in the scheduling of cleaning operations, and to support the

development of guidelines for exchanger and network retrofitting.

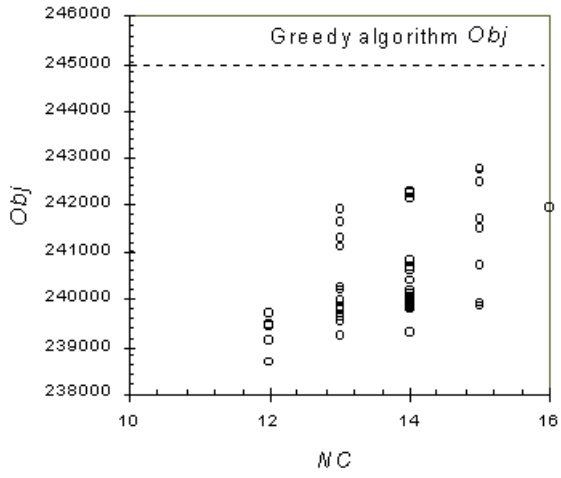

Fig. 1 Distribution of solutions generated by a refinery scheduling study over a 3 year operating horizon (Smaïli *et al*. 2001). The dashed line, labelled 'greedy algorithm', is the result of a simple 'floating horizon' approach: points show optima generated by their MINLP method. *Obj* is the objective function, here in £: *NC* is the number of cleaning actions. Constant flow rate scenario.

THE IMPACT OF FOULING ON NETWORKS

Thermal impact

In the absence of detailed information, the fouling deposit is treated as a uniform layer of thickness δ and thermal conductivity λ_f. For tubeside fouling, which is the case considered here, the thermal impact is expressed via the fouling resistance, R_f, which Yeap *et al*. (2004) have shown to be reasonably well described by the 'thin-slab' approximation for PHT applications:

$$R_f \approx \frac{\delta}{\lambda_f} \tag{1}$$

where R_f is related to the overall heat transfer resistance, U, by

$$\frac{1}{UA_{i,c}} = \frac{1}{A_{i,f}h_i} + \frac{1}{A_o h_o} + \frac{R_f}{A_{i,c}} + \frac{R_W}{A_o} \approx \frac{1}{(UA)_{i,c}} + \frac{R_f}{A_{i,c}} \tag{2}$$

where $A_{i,c}$ the internal clean surface area, $A_{i,f}$ the internal surface area after fouling and $A_{o,c}$ the outer surface area of the HE. In network simulations we use the *NTU*-effectiveness (*e*) method to calculate the performance of the exchanger. *NTU* is defined as

$$NTU = \frac{UA}{W_{\min}} \tag{3}$$

where $W_{\min}$ is the smaller of the heat capacity flow rates in the unit. The effect of fouling on performance depends on the initial value of *NTU*: large values make *e* less sensitive to changes in *NTU* – which is how adding excess area to counter fouling 'works' (but it simply disguises the thermal effect: the hydraulic one cannot be disguised). Changes in *NTU* can be quantified by the fouling Biot number, Bi_f, which is defined as,

$$Bi_f = U_{clean} R_f \tag{4}$$

and when $A_{i,c} \sim A_{i,f}$,

$$\frac{NTU}{NTU_{clean}} = \frac{(UA)_{clean}}{(UA)_{clean} + U_{clean}R_f} \approx \frac{1}{1+Bi_f} \tag{5}$$

The impact on network performance of fouling in a particular exchanger can then be gauged by the change in *e* resulting from a given extent of fouling, in a manner similar to the 'sensitivity table' analysis described by Kotjabasakis and Linnhoff (1986). Conversely, the value of R_f required to change *e* significantly (say, by 10%) can be calculated via the *NTU-e* relations and Eq. (5). Let this critical value, R_f^*, correspond to a foulant thickness, δ_{th}, such that $R_f^* = \delta_{th}/\lambda_f$. If the expected fouling rate in an individual unit is known or can be estimated based on the initial operating conditions, the impact of fouling can be compared between exchangers in a network in terms of a *characteristic time*, Δt_{th}, for fouling to cause problems. Ignoring variations caused by changes in geometry and temperature, the critical Bi_f^* and R_f^* values will be reached after Δt_{th} calculated thus:

$$\begin{aligned} Bi_f^* &= U_{clean} R_f^* = U_{clean} \left.\frac{dR_f}{dt}\right|_0 \Delta t_{th} \\ \Rightarrow \Delta t_{th} &= R_f^* \Big/ \left.\frac{dR_f}{dt}\right|_0 \end{aligned} \tag{6}$$

Hydraulic impact

The tubeside pressure drop across an exchanger increases due to fouling (i) changing the roughness of the fluid-tube interface; (ii) reducing the cross-sectional area available for flow; and (iii) potentially blocking tubes and causing flow maldistribution. Ignoring (iii), the pressure drop is given by

$$\begin{aligned} \Delta P &= \Delta P_{ends} + \Delta P_{tubes} \\ &\approx a \cdot \dot{m}^2 + b \cdot \dot{m}^{1.75\sim 2} \cdot (d_t - 2\delta)^{-4.75\sim 5} \end{aligned} \tag{7}$$

where m is the mass flow rate and d_t is the tube i.d. ΔP is therefore roughly proportional to m^2 and very sensitive to changes in duct size (a δ/d_t value of 0.06 will double

ΔP_{tubes}). The primacy of the thermal conductivity in Eq. (1) is now evident, as $\delta \sim R_f \lambda_f$. For crude oil fouling, λ_f is expected to lie between that of the oil and an amorphous coke (~ 0.1-2 W/m K; Watkinson, 1988). Figure 2 shows that λ_f determines whether the primary impact of fouling on an individual exchanger will be hydraulic or thermal.

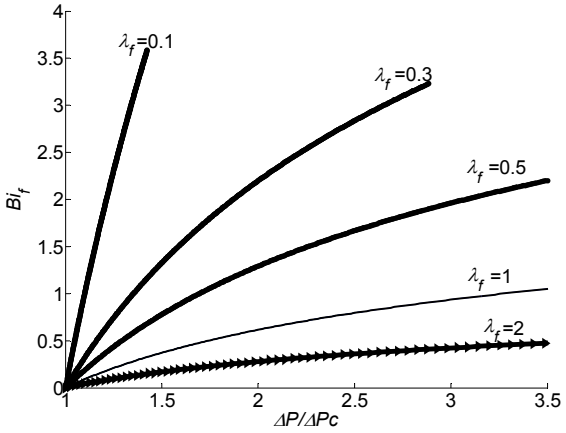

Fig. 2 Impact of fouling on thermal and hydraulic performance (ΔP_{tubes}), for different λ_f values.

A characteristic operating time for hydraulic impact can be defined in a similar manner to that above, based on the thickness of the fouling layer required to increase the tubeside pressure drop by a predetermined amount, assuming constant flow rates and a fouling rate based on initial conditions. The corresponding critical deposit thickness, δ_{hy}, will be related to a fouling resistance via $\delta_{hy} \sim R_f^* \lambda_f$ and therefore

$$\Delta t_{hy} = \frac{\delta_{hy}}{\lambda_f} \Big/ \left. \frac{dR_f}{dt} \right|_0 \qquad (8)$$

Comparing these two characteristic times gives

$$\frac{\Delta t_{th}}{\Delta t_{hy}} = \frac{\lambda_f}{\delta_{hy}} R_f^* = \frac{\delta_{th}}{\delta_{hy}} \qquad (9)$$

It follows from Figure 2 that low values of λ_f will result in the thermal limitation being met before the hydraulic limitation and vice versa.

Illustration: fouling feedback or thermo-hydraulic channelling

The importance of λ_f is demonstrated by comparing two notionally identical exchangers operating in parallel as shown in Figure 3 and summarized in Table 1. Tubeside fouling is simulated using the fouling model reported by Polley *et al*. (2002), Eq. (10), so that the fouling rate varies with temperature and flow rate. The flow to the splitter at A is held constant while the (common) pressure drop across the exchangers is increased in order to counter the hydraulic effects of fouling. The hot stream flow and split are held constant. Exchanger 2 is set to have a slightly fouled initial condition (R_f = 0.01 m^{2}K/kW, or Bi_f = 0.00463) in order to differentiate the two exchangers. The characteristic operating times calculated for the thermal and the hydraulic constraints are listed in Table 1. These give a rough indication of the value of λ_f which would shift the heat exchanger (HE) performance limitation from thermal to hydraulic (about 0.45 W/ m K for this case).

$$\frac{dR_f}{dt} = A_f \, \mathrm{Re}^{-0.8} \, \mathrm{Pr}^{-0.33} \exp\left(\frac{-E}{RT_s}\right) - Cu^{0.8} \qquad (10)$$

where A_f = 3.7 $\times 10^6$ m^{2}K/kW h, E = 55 kJ/mol, and C = 3.2 $\times 10^{-7}$ m^2/kW h Pa.

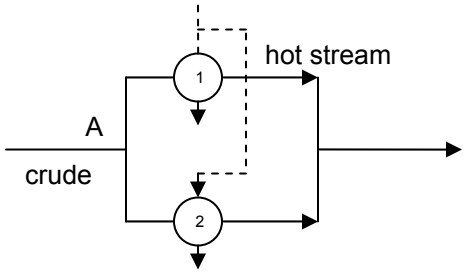

Fig. 3 Two nearly identical heat exchangers in parallel. (HE2 initially slightly fouled).

Figure 4 shows the impact of fouling over one year of operation. The timescale is secondary and depends on the fouling rates. The hydraulic effect is noticeable at a later stage than one might expect from the characteristic thermal time because the fouling rate changes over time. The plots show that higher fouling can cause a flow imbalance between the two exchangers – a hydraulic effect - which accelerates fouling in the exchanger with the lower flow rate. This hydraulic feedback is very strong at larger λ_f values: the imbalance reinforces thermal fouling and eventually the system becomes inoperable. With lower λ_f values, the increase in pressure drop is not large enough to cause an imbalance and the thermal effect dominates.

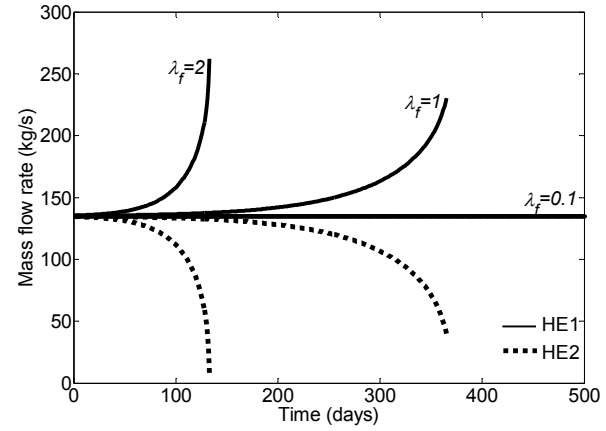

(a)

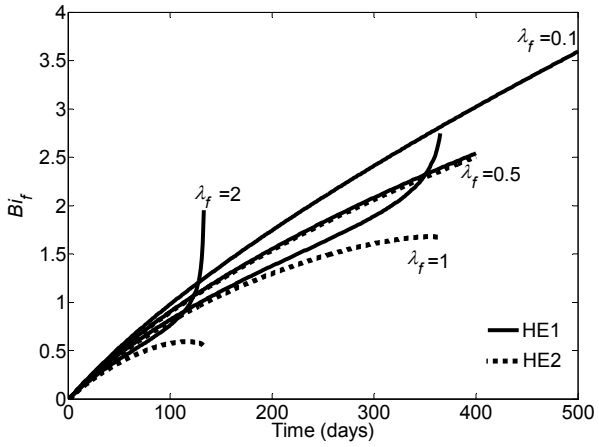

(b)

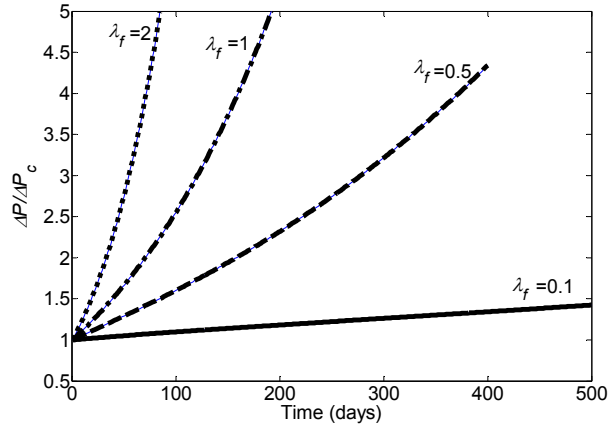

(c)

Fig. 4 Effect of λ_f on (a) divergence of mass flow rate, (b) fouling Biot number, (c) increase in ΔP_{tubes}.

Hydraulic impact in networks

The maximum pressure drop in a refinery PHT is set by design codes which inhibit the use of operating pressures above 40 bara; a common pressure drop limit is 300 psi (20.7 bar) (Shell, 2007). This energy is dissipated across heat exchangers, piping, control valves *etc*. so that the impact of fouling on the network pressure drop is smaller than that suggested by Eq. (7). This behaviour needs to be accounted for if the throughput is to be allowed to vary. We introduce a pressure distribution factor, α, to quantify this distribution based on clean operation at the target flow rate, *viz*.

$$\alpha = \frac{\Delta P_{piping}}{\Delta P_{HEX,clean}} \tag{11}$$

The piping component in the numerator will be roughly $\propto \dot{m}^2$, as is the first term in Eq. (7). Practical cases probably involve α values in the range $0.3 < \alpha < 3$. The impact of control valves, which are opened as the pressure drop increases, is modelled as shown in Figure 5. The centrifugal pump will be capable of delivering a larger flow than the target value, $\dot{m}^*$, until fouling causes the network characteristic to reach D. At this point the control valve on the line will be fully open and the flow rate will be determined by the pump characteristic. The combined characteristic features a discontinuity of slope which is incorporated in the simulation.

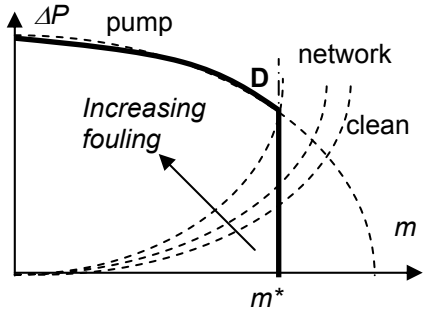

Fig. 5 Preheat train hydraulic operation: combined characteristic curve in bold

NETWORK SIMULATION

The governing heat transfer and hydraulic relationships presented by Smaïli *et al*. (2001) have been incorporated along with the above components in to a simulation using MATLAB™/Excel™. Its implementation is demonstrated using the network shown in Figure 6. The target throughput is 95 kg/s (~62,000 bbl/day); its clean performance is summarized in Table 2. The pump characteristic is based on an overdesign of 5%. A λ_f value of 0.2 W/m K was used: the constant fouling rates used were based on the original paper.

The estimates of Δt_{hy} and Δt_{th} indicate that HE3 is unlikely to face thermal limitations over the 3 year operating period: this is confirmed by the cleaning schedules presented later. Variable throughput requires the hot stream mass flows to be proportional to the cold stream flow rate; changes in film heat transfer coefficients are also evaluated. Fouling is assumed to occur only on the crude (tube) side. Calculations were performed on an AMD Athlon™ 64 Processor 2.41 GHz PC with 2 GB RAM.

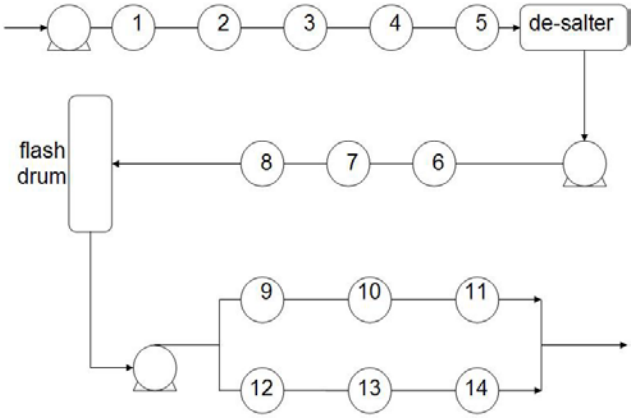

Fig. 6 Arrangement of 14 heat exchangers in the case study PHT network, after Smaïli *et al*. (2001). HE specifications given in Table 2.

Figure 7 shows the performance of the network over the 3 year period for the case where no cleaning is performed. Excellent agreement with the original reported results was obtained for operation at constant mass flow rate. The plots highlight the importance of hydraulic impact, which is greatest at low α, *i.e*. when the pressure drop across the exchangers dominates the total pressure drop. The reduction of throughput, by some 21,000-306,000 te over 3 years, is significant: at a marginal cost of 5 US$/bbl (Shell, 2007), this represents a lost opportunity of 0.8-11.3M US$.

Cleaning complications

Isolating individual exchangers for cleaning is a frequently practiced mitigation method but while the unit is out of service, the drop in heat transfer duty can be excessive unless some flow split optimization is performed. Likewise, throughput can temporarily increase owing to the absence of the fouled exchanger. These dynamics are considered here by optimizing the flow splits, within predetermined limits, during each operating period. The algorithm is set to maximize throughput first, with energy recovery as a secondary criterion. For example the fraction of flow through each leg at the hot end of the PHT, *i.e*. HE 9-11 and 12-14, is allowed to vary between 0.4 and 0.6 of the maximum, initial throughput, representing operation up to the design limit of the exchangers.

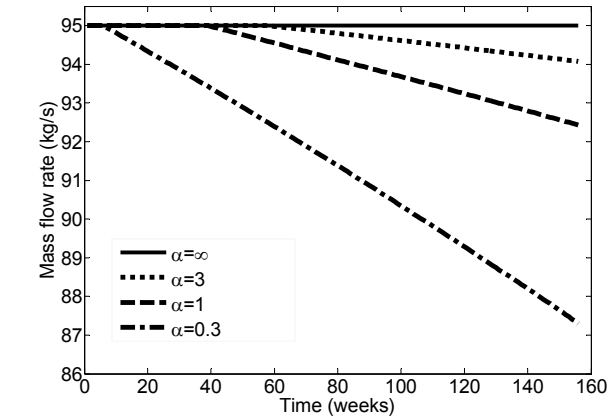

(a)

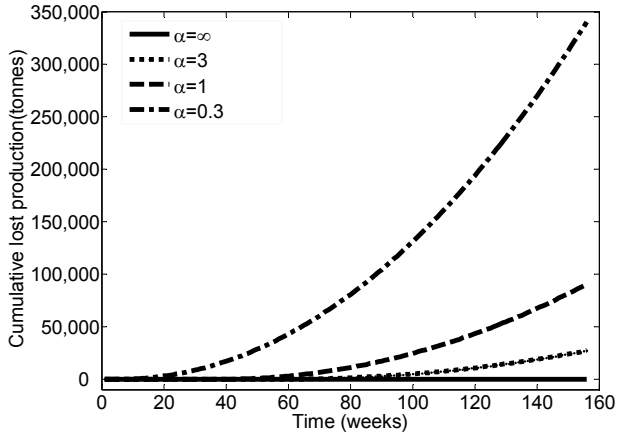

(b)

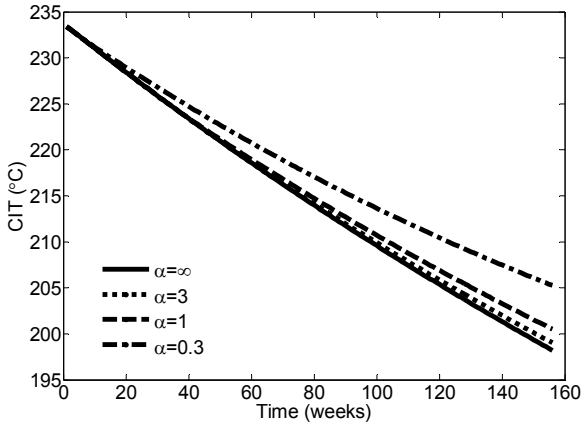

(c)

Fig. 7 Effect of α on case study network, no cleaning.

In a rigorous optimization of the cleaning schedule, all exchangers would be considered at the evaluation stage, with commensurate cost in computational time. The search space is therefore shrunk by using impact criteria which denote when a unit is to be considered for cleaning: a thermal impact, β_E

$$\beta_E = e_c - e \tag{12}$$

and hydraulic impact, β_P

$$\beta_P = \frac{\Delta P_f}{\Delta P_c} \tag{13}$$

where the values of β_t may vary from one exchanger to another depending on its design specification, or on network targets such as run-down temperatures and pumparound duty. A further condition to be satisfied before considering a unit for cleaning is constructed by estimating the financial benefit of cleaning and comparing this with a threshold value, Δ_G (typically a multiple of the cost of the cleaning operation). The improvement in heat transfer and throughput on cleaning is estimated and is assumed to remain constant over the time horizon Δt_G following cleaning (which may be a fixed period, such as 1 year, or the time left until the next shutdown), yielding the criterion,

$$\left\{C_{lo}\left(\dot{m}_c - \dot{m}_f\right) + C_E \beta_E Q_{\max}^{clean}\right\}\Delta t_G > \Delta_G \tag{14}$$

where C_{lo} is the cost of lost opportunity and C_E the energy cost. The transient in throughput and heat transfer during the cleaning period is not considered at this stage; Eq. (14) simply considers the benefit in the refurbished state. Exchangers which satisfy these constraints are then compared using a detailed simulation over the horizon and the full, integral form of the objective function, G, Eq. (15) is evaluated.

$$\begin{aligned} & G_m\Big|_{period\ \mathrm{j}} \\ & = \int_{t_j}^{t_{j+N_S}} C_E\left\{Q(t)\Big|_{no\ \text{cleaning}} - Q(t)\Big|_{\text{clean m in period j}}\right\}dt \\ & + \int_{t_j}^{t_{j+N_S}} C_{lo}\left\{\dot{m}(t)\Big|_{clean\ \text{m in period j}} - \dot{m}(t)\Big|_{no\ \text{cleaning}}\right\}dt \\ & - C_{c,m} \end{aligned} \tag{15}$$

The time horizon is divided into intervals of equal length and the heat exchanger giving the highest positive value of G_m is selected for cleaning. Only one exchanger is cleaned at a given time, in accordance with most refineries' practice between shut-downs.

The network fouling penalty function is evaluated using Eq. (16) and can be used to evaluate different scenarios, such as the benefit of instructing cleaning compared to taking no cleaning action.

$$Obj = \int_0^{t_f} Q(t)C_E + C_{lo}\left(\dot{m}_{\text{target}} - \dot{m}(t)\right)dt + N_c \cdot C_{c,m} \tag{16}$$

CASE STUDY

The PHT network in Figure 6 has parallel trains at the hot end of the system. Any of the exchangers can be removed for cleaning. Two cost structures are investigated, with different energy costs and common factors C_{lo} - 5 US$/bbl (or 37 US$/te) and C_c - 5000 $/clean: cost structure A - C_E = 6.5 US$/MBtu (or 0.592 US$/kW day); B (cheaper energy) C_E -1 US$/MBtu (or 0.091 US$/kW day). Three scenarios are compared under this case study, namely

I. Operation without cleaning (base case)
II. Operation with cleaning without flow split control (constant flow split)
III. Operation with cleaning and flow split control (flow split control set to maximize throughput and then maximize heat recovery)

The PHT operates continuously for a 3 year period followed by a shutdown, with $\alpha = 1$. A greedy algorithm threshold value of 2000 US$ was used. Time was discretized in one month intervals with one week sub-periods for cleaning: a sliding time horizon, Δt_G, of 6 months was used and the period after shutdown of the network was not considered, *i.e.* as shutdown approached, Δt_G shortened. The furnace coil outlet temperature (used to calculate the furnace duty) was set at 363°C to determine the heat duty imposed on the furnace.

The results for the three case studies under two cost factors are summarized in Figures 8 and 9 and Table 3. The importance of the flow split optimization is evident. The influence of the cost structures on throughput and the scheduling of cleaning, and consequently on the entire return, are also evident.

DISCUSSION

The new simulator worked successfully, and the base case scenario results matched those reported by Smaïli *et al*. The response of flow rates to the progress of fouling was represented, instead of assuming constant throughput, thereby extending the previous work.

The optimized schedules in Figure 9 proved to be very sensitive to the cost structure, in particular to the relative costs of the lost profit opportunity consequent on reduced throughput, and the energy costs incurred from sending a cooler stream to the furnace.

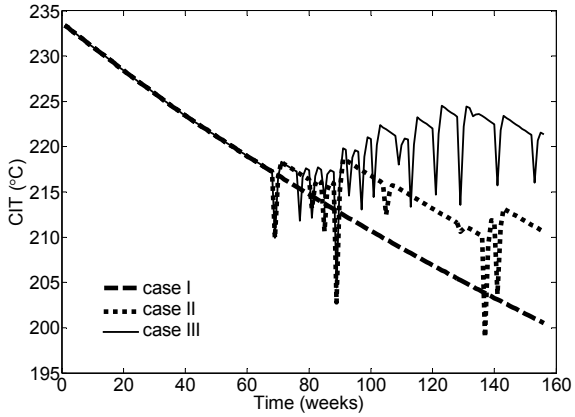

(a-A)

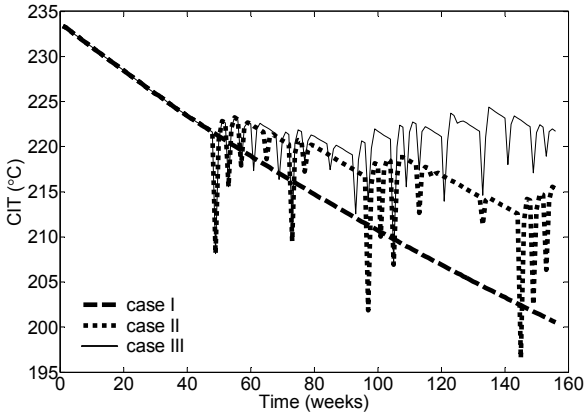

(a-B)

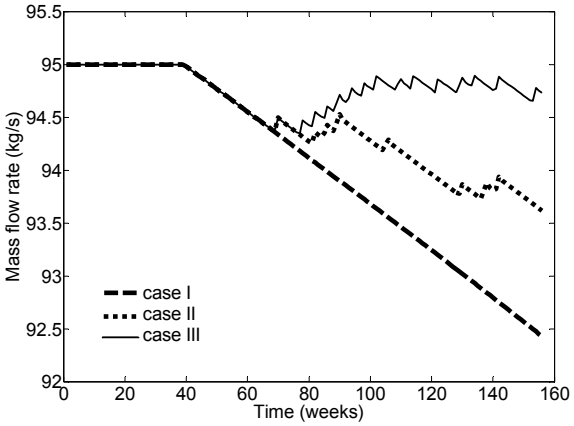

(b-A)

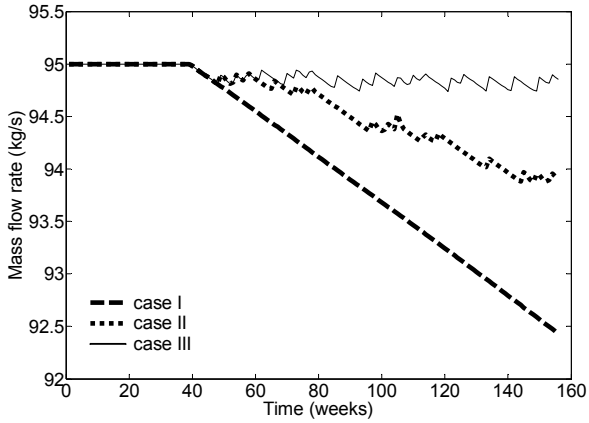

(b-B)

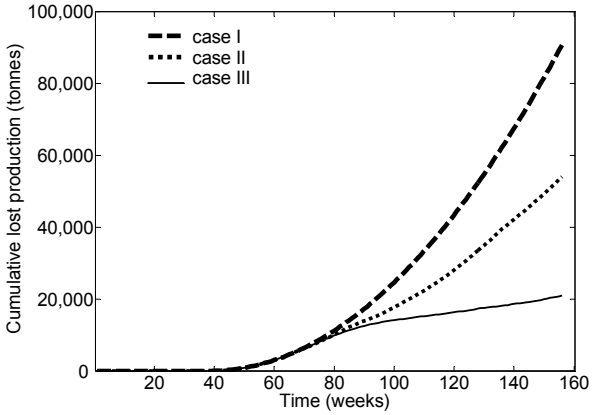

(c-A)

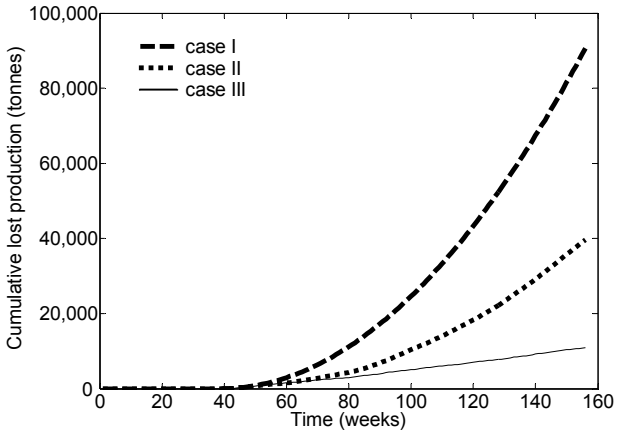

(c-B)

Fig. 8 Performance of case study PHT for scenarios I-III with cost structures A and B; (a) CIT (b) throughput, (c) cumulative lost production.

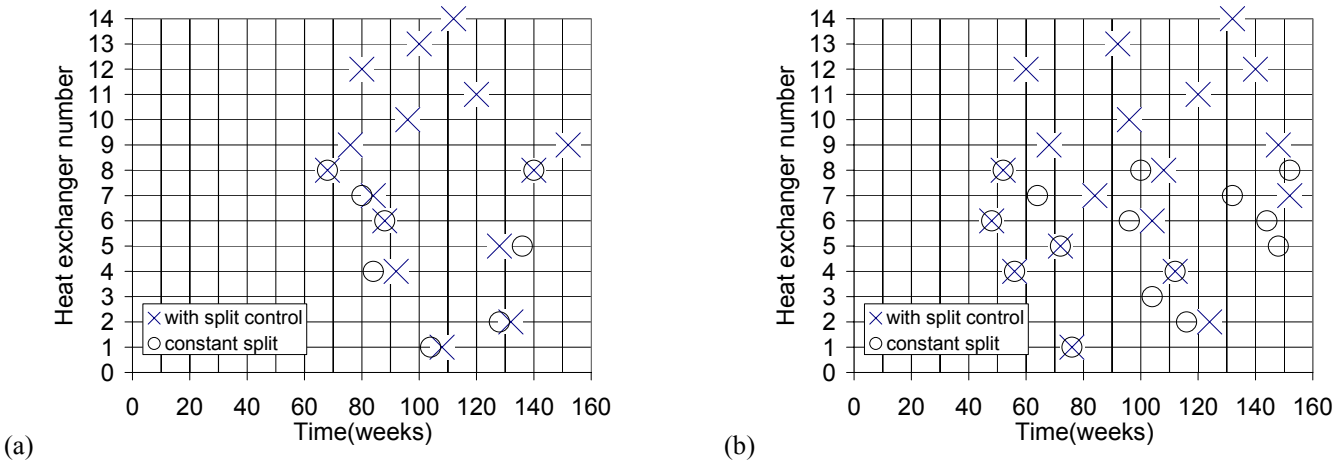

Fig. 9 Cleaning schedule for scenarios II and III with cost structure (a) A and (b) B.

Under both cost structures, both scenarios II and III show a decline in heat recovery and throughput until there sufficient economic benefit to start cleaning. Figure 8 shows that the onset of cleaning – the mitigation strategy being considered in this work – is started at different times depending on the cost structure. Cost structure A seeks to maximize energy recovery and cleaning starts later; cleaning also stops earlier as the period available for recovering energy (and balancing the penalty incurred during the cleaning sub-period) is reduced as shutdown approaches. The latter feature is observed in most scheduling studies which consider fixed time horizons. Cost structure B gives more emphasis to throughput and the PHT is operated noticeably differently: cleaning is started earlier, once fouling causes the hydraulic limit to be reached, and continues up to the shutdown in order to maximize throughput (Figure 8(b)). The two cost structures effectively demonstrate the difference between energy- and throughput-dominated management strategies.

Figure 9 shows that the network is cleaned often, which operators may view as *too* often. This is due to the cost structure: an increase in C_c will reduce the frequency. It should also be noted that constant, linear fouling rates have been used in this case study and the implementation of fouling rate models sensitive to local conditions will give more realistic results as the fouling rates will generally decrease as the crude temperature decreases.

The effect of manipulating the flow splits during and following cleaning actions is evident from comparing scenarios II and III. The improvement in performance is noticeable, both in terms of throughput and CIT. Flow split manipulation improves the attractiveness of a cleaning-based mitigation strategy, and installing equipment to allow flow manipulation represents a reasonably cheap retrofitting option. Furthermore, comparison of the schedules for individual exchangers in Figure 9 indicates that that units 6-8 are cleaned quite often, and a cleaning-based strategy may benefit from replacing these units by two exchangers in parallel. Alternatively, an extra exchanger could be added and held on standby to handle the duty while one of these units is off-line being cleaned.

CONCLUSIONS

An analysis of the thermal and hydraulic impacts of fouling has been presented. For fouling rate laws that incorporate the threshold fouling concept, characteristic times for fouling of an exchanger were identified, based on hydraulic or thermal limitations. The importance of the foulant thermal conductivity has been identified and the need for accurate values of this parameter highlighted.

The interaction between thermal and hydraulic effects has been shown to give rise to thermo-hydraulic channelling under certain conditions: the deleterious impact of this phenomenon has been demonstrated using a simple example.

MATLAB™/Excel™ has been used to construct a highly flexible simulator intended to support the development of guidelines for exchanger and network retrofitting. The code includes the characteristics generated by constant-speed centrifugal pumps operating with control valves, and the change in throughput resulting from saturating the control valve. The cleaning scheduling algorithm includes a filtering heuristic to reduce the computational demands of the calculations, which were performed using the 'greedy algorithm'.

The simulator has been tested successfully for the scheduling of cleaning operations. Simulated PHT performance has been improved by manipulating flow splits as fouling proceeds. The resultant cleaning

schedules are sensitive to the cost structure, which can be simply set to favour throughput over energy recovery.

Acknowledgements
Funding from the EPSRC (EP/D50306X) is gratefully acknowledged, as are helpful discussions with staff at Shell, bp, ConocoPhillips and Dr Graham Polley.

NOMENCLATURE

a constant, kg/m^3 s^2
b constant, m$^{4.75\sim5}$/ kg$^{1.75\sim2}$
A heat transfer area, m^2
A_f constant, m^{2}K/kW h
Bi_f Biot fouling number, -
C constant, m^2/kW h Pa
C_C cost of cleaning heat exchanger, US$/clean
C_E Energy cost, US$/kW
C_{lo} Lost opportunity cost, US$/kg
C_P specific heat capacity
CIT coil inlet temperature, °C
d_t tube internal diameter, m
e effectiveness, -
E_{II} activation energy, J/ mol
G_m return on cleaning unit m, US$
h heat transfer coefficient, W/m^2 K
$\dot{m}$ mass flow rate, kg/s
N_c number of cleaning actions, -
N_P number of periods, -
N_S number of periods in greedy algorithm horizon, dimensionless
NTU number of transfer units, -
Pr Prandlt number, -
Q furnace or exchanger heat duty, kW
R gas constant, J/mol K
R_f fouling resistance, m^{2}K/W
R_W wall resistance, m^{2}K/W
Re Reynolds number, -
T temperature, K
t time, day
t_f time at end of cleaning horizon, day
T_S surface temperature, K
U overall heat transfer coefficient, W/m^2 K
u tube velocity, m/s
W_{min} smaller heat capacity flow rate, W/K

Greek letters

α pressure distribution ratio, -
β_E effectiveness difference, -
β_P pressure drop ratio of HEX reference to clean state, -
δ thickness of the deposition layer, m
δ_{hy} critical thickness (deposition) for hydraulic limit, m
δ_{th} critical thickness (deposition) for thermal limit, m
ρ density, kg/m^3
λ_f thermal conductivity of the foulant layer, W/m K
Δ_G greedy threshold value, US$
ΔP pressure drop, N/m^2
Δt_{hy} characteristic hydraulic time, day
Δt_{th} characteristic thermal time, day
Δt_G sliding time horizon, day

Subscripts

c	clean state
ends	at the tube ends, headers *etc*.
f	fouled state
i	internal
o	outer
tubes	across the tubes

Superscripts

c cold stream
h hot stream
in inlet

REFERENCES

Angadi, D., Hatch, C.M., Smaïli, F., Herbert, O., Vassiliadis, V.S. & Wilson, D.I., 1999, 'Optimisation of cleaning schedules in heat exchanger networks: Sugar refinery case study', *TransIChemE Part C,* 77, 159-164.

Ebert, W. and Panchal, C.B., 1997, Analysis of Exxon crude-oil slip stream coking data, in *Fouling Mitigation of Industrial Heat Exchange Equipment*, Panchal, C.B., Bott, T.R., Somerscales, E.F.C. and Toyama, S. (eds.), Begell House, NY, 451-460.

ESDU (Engineering Sciences Data Unit), 2000, Heat exchanger fouling in the preheat train of crude oil distillation levels, *Data Item 0016*, ESDU Intl., London.

Georgiadis, M.C, Papageorgiou, L.G, and Macchietto, S., 2000, 'Optimal energy and cleaning management in heat exchanger networks under fouling, *Ind. Eng. Chem. Res*., *39*, 441-454.

Kotjabasakis, E. and Linnhoff, B., 1986, Sensitivity tables for the design of flexible processes. I. How much contingency in heat exchanger networks is cost-effective?, *Chem. Eng. Res. Des*., Vol. 64, 197.

Lavaja, J.H. and Bagajewicz, M.J., 2004/5, *Ind. Eng. Chem. Res*., 43, 3924-3938; 44, 8046-8056; 8136-8146.

Polley G.T., Wilson D.I., Yeap B.L. and Pugh S.J., 2002, Use of crude oil fouling threshold data in heat exchanger design, *Appl. Thermal Eng.*, Vol. 22, pp. 763-776.

Sanaye S., Niroomand B., 2007, Simulation of heat exchanger network (HEN) and planning the optimum cleaning schedule, *Energy Conservation and Design*, Vol. 48, pp 1450-1461.

Shell Global Solutions, 2007, Personal communication.

Smaïli F., Vassiliadis V.S. and Wilson D.I., 2001, Mitigation of fouling in refinery heat exchanger networks by optimal management of cleaning, *Energy & Fuel*, Vol. 15, pp. 1038-1056.

Watkinson A.P., 1988, Critical review of organic fluid fouling: final report, *ANL/CNSV-TN-208*, Argonne National Laboratory, p111

Wilson, D.I., Polley, G.T. and Pugh, S.J., 2005, Ten years of Ebert, Panchal and the 'threshold fouling' concept, in *Proc*. Heat Exchanger Fouling and Cleaning: Challenges and Opportunities, Kloster Irsee, Germany. http://services.bepress.com/eci/heatexchanger2005/6.

Yeap B.L., Wilson D.I., Polley G.T. and Pugh S.J., 2004, Mitigation of crude oil refinery heat exchanger fouling through retrofits based on thermo-hydraulic fouling models, *Chem. Eng. Res. Des*, Vol. 82(A1), pp. 53-71.

Yeap, B.L., Wilson, D.I., Polley, G.T. and Pugh, S.J. (2005) Retrofitting crude oil refinery heat exchanger networks to minimise fouling while maximising heat recovery, *Heat Transfer Engineering*, **26**(1), 23-34.

Table 1 Details of the heat exchanger system in Figure 3

HE Number	λ_f (W/m K)	Δt_{hy} [a] (days)	Δt_{th} [b] (days)	U_{clean} (W/m^{2}K)	R_f (initial) (W/m^{2}K)	Surface Roughness (m)	Initial fouling rate (m^{2}K/kWday)	Area (m^2)
1	0.1 0.5 1 2	108 22 11 5	26	463	(1) 0 (2) 0.00001	0.000043	0.018	477

[a] $\Delta t_{c,hy}$ calculated on basis of $\Delta P / \Delta P_{clean}$ reaching 1.1; [b] $\Delta t_{c,th}$ calculated on basis e decreasing by 10%.

Table 2 Summary of heat exchanger details, clean operation

Unit	$T^{h,in}$ °C	$T^{c,in}$ °C	m^h kg/s	m^c kg/s	C_P^h kJ/kg K	U_{clean} W/m^2 K	A m^2	Linear fouling rate $\times 10^{11}$ m^{2}K/J	Δt_{hy} days	Δt_{th} days	Cleaning Cost US$	Cleaning Time days
1	194	26	19.1	95	2.8	500	56.6	0.6	1696	522	5000	7
2	296	45	3.3	95	2.9	500	8.9	0.9	1699	366	5000	7
3	197	50	55.8	95	2.8	500	208.3	0.6	1686	757	5000	7
4	170	101	49.7	95	2.8	500	112.9	0.8	1302	451	5000	7
5	237	116	49.7	95	2.9	500	121.6	0.8	1201	463	5000	7
6	285	135	34.8	95	2.8	500	110.1	1.5	654	255	5000	7
7	205	161	55.8	95	2.9	500	67.2	1.1	923	283	5000	7
8	254	167	45.5	95	2.6	500	67.1	1.5	677	210	5000	7
9, 12	249	178	9.5	46	2.8	500	91	2.5	416	290	5000	7
10,13	286	191	22.8	46	2.6	500	61.3	1.8	537	206	5000	7
11,14	334	210	17.4	46	2.6	500	55.6	1.9	603	203	5000	7

Table 3: Summary of case study PHT performance under different operational strategies

Scenario	I		II		III	
Cost Structure	A	B	A	B	A	B
Average CIT (°C)	216.0	216.0	218.6	219.0	222.0	222.7
Average throughput (kg/s)	94.0	94.0	94.4	94.6	94.8	94.9
Number of cleaning actions	0	0	8	15	15	19
Objective function (M US$)	22.2	6.3	20.6	4.3	18.3	3.2
Average heat duty delivered by the network (MW)	40.5	40.5	41.3	41.6	42.1	42.3